

Requirement for *Dlgh-1* in Planar Cell Polarity and Skeletogenesis during Vertebrate Development

Charlene Rivera¹[¶], Sara J. S. Simonson²[¶], Idella F. Yamben¹[¶], Shalini Shatadal¹, Minh M. Nguyen¹[¶], Maryline Beurg³, Paul F. Lambert², Anne E. Griep¹*

1 Department of Cell and Regenerative Biology, University of Wisconsin-Madison, Madison, Wisconsin, United States of America, **2** Department of Oncology, University of Wisconsin-Madison, Madison, Wisconsin, United States of America, **3** Institut National de la Santé et de la Recherche Médicale, Hôpital Pellegrin, Bordeaux, France

Abstract

The development of specialized organs is tightly linked to the regulation of cell growth, orientation, migration and adhesion during embryogenesis. In addition, the directed movements of cells and their orientation within the plane of a tissue, termed planar cell polarity (PCP), appear to be crucial for the proper formation of the body plan. In *Drosophila* embryogenesis, *Discs large* (*dlg*) plays a critical role in apical-basal cell polarity, cell adhesion and cell proliferation. Craniofacial defects in mice carrying an insertional mutation in *Dlgh-1* suggest that *Dlgh-1* is required for vertebrate development. To determine what roles *Dlgh-1* plays in vertebrate development, we generated mice carrying a null mutation in *Dlgh-1*. We found that deletion of *Dlgh-1* caused open eyelids, open neural tube, and misorientation of cochlear hair cell stereociliary bundles, indicative of defects in planar cell polarity (PCP). Deletion of *Dlgh-1* also caused skeletal defects throughout the embryo. These findings identify novel roles for *Dlgh-1* in vertebrates that differ from its well-characterized roles in invertebrates and suggest that the *Dlgh-1* null mouse may be a useful animal model to study certain human congenital birth defects.

Citation: Rivera C, Simonson SJS, Yamben IF, Shatadal S, Nguyen MM, et al. (2013) Requirement for *Dlgh-1* in Planar Cell Polarity and Skeletogenesis during Vertebrate Development. PLoS ONE 8(1): e54410. doi:10.1371/journal.pone.0054410

Editor: Xin Zhang, Indiana University School of Medicine, United States of America

Received: June 20, 2012; **Accepted:** December 13, 2012; **Published:** January 22, 2013

Copyright: © 2013 Rivera et al. This is an open-access article distributed under the terms of the Creative Commons Attribution License, which permits unrestricted use, distribution, and reproduction in any medium, provided the original author and source are credited.

Funding: This work was supported by NIH grants EY09091 (AEG), CA908428 (PFL/AEG). The University of Wisconsin Carbone Cancer Center (P30 CA14520) provided shared service support for the project. The funders had no role in the study design, data collection and analysis, decision to publish or preparation of the manuscript.

Competing Interests: The authors have declared that no competing interests exist.

* E-mail: aegriep@wisc.edu

[¶]a Current address: Lineberger Comprehensive Cancer Center, University of North Carolina, Chapel Hill, North Carolina, United States of America

[¶]b Current address: Center for Commercialization, University of Washington, Seattle, Washington, United States of America

[¶]c Current address: Kelly Scientific Resources, Madison, Wisconsin, United States of America

[¶]d Current address: Lillehei Heart Institute, University of Minnesota School of Medicine, Minneapolis, Minnesota, United States of America

[¶] These authors contributed equally to this work.

Introduction

The development of specialized organs in vertebrates is tightly linked to the regulation of cell growth, apical-basal cell polarity and cell-cell adhesion during embryogenesis. In addition, the directed movements of cells and their orientation in the same direction within the plane of a tissue, termed planar cell polarity (PCP), appear to be crucial for the proper formation of the body plan. Of great interest has been to decipher the mechanisms involved in regulating these critical aspects of development. From studies in invertebrates it is known that certain PSD95/*Dlg*/*ZO-1* (PDZ) domain containing proteins such as Discs-large (*Dlg*) play prominent roles in regulating apical-basal polarity [1,2] while different PDZ proteins are part of a genetic network that regulates PCP [3]. Recent work in vertebrates supports the contention that the function of many polarity factors has been conserved cross-species. However, studies also suggest that certain factors have different or additional roles in vertebrates as compared to invertebrates [4]. In this study, we address the role of *Dlgh-1*, the mouse homolog of *Drosophila dlg*, in mouse development.

In *Drosophila melanogaster*, mutations in *dlg* and *scrib*, the gene encoding a second PDZ protein, Scribble, result in neoplastic

overgrowth, multilayering and loss of cell shape in various epithelial tissues including the imaginal discs [1], the embryonic epidermis, and the follicular epithelia [2], suggesting a role for these factors in cell proliferation, adhesion and apico-basal polarity. In *Drosophila* and *Caenorhabditis elegans*, *Dlg* and *Scrib* are thought to be required for properly localizing and maintaining adherens junctions and apical determinants [1,2,5,6,7,8,9]. In *Drosophila*, *Dlg* localizes to the septate junctions where it forms a complex with *Scrib* and Lethal giant larvae (*Lgl*) [1,2]. This *Dlg*/*Scrib*/*Lgl* complex antagonizes other PDZ complexes, thereby restricting adherens junctions and apical determinants, such as *Crumbs*, to the appropriate compartment [10]. Finally, the Partner of *Inscuteable*/*Discs-large* complex is required for planar polarity during the asymmetric division of the sensory organ precursor (*pl*) cell [11].

Dlg is a member of the membrane-associated guanylate kinase (MAGUK) family [12], and, as a scaffolding protein, is capable of assembling supramolecular complexes at specific sites within and proximal to the cytoplasmic membrane. *Dlg* may accomplish this by interacting with other molecules through its multiple protein-protein interaction domains, which include three PDZ domains, a src-homology 3 (SH3) domain, a band 4.1 domain, and

a guanylate kinase homolog (GUK) domain [12]. Homologs of *Drosophila* Dlg are found in humans (hDlg), rat (SAP97), and mouse (Dlgh-1, also referred to as Dlg-1), and the high degree of conservation among its multiple domains suggests conserved function cross-species [13,14,15]. In mammals, Dlgh-1 is ubiquitously expressed and is found at sites of cell-cell contacts in epithelial and neuronal cells [16,17,18,19,20,21]. It interacts with a wide variety of proteins, which include the tumor suppressors adenomatous poly (APC) [22] and protein tyrosine phosphatase and tensin homologue (PTEN) [23], Shaker-type K⁺ channel α -subunits [24], the G-protein coupled receptor homologue tumor endothelial marker 5 (TEM5) [25], and the MAGUK Lin-2/CASK [26]. In addition to interacting with endogenous cellular proteins, Dlgh-1 is also targeted by multiple human viral oncoproteins including the human papillomavirus (HPV) E6 [27], the adenovirus E4-ORF1 [28], and the human T cell leukemia virus type 1 (HTLV-1), Tax 1, [29]. These interactions have been implicated in the transforming and tumorigenic properties of the viral oncoproteins [27,29,30,31,32,33].

The role of *Dlgh-1* in mouse development has begun to be explored. Caruana and Bernstein [34] reported that mice carrying a gene trap insertion in *Dlgh-1* (*Dlgh-1^{gt/gt}* mice), which results in a Dlgh-1 protein lacking the SH3, band 4.1, and GUK domains, exhibited a cleft palate and a shorter mandible than *Dlgh-1* wild type mice. Additional studies on this *Dlgh-1^{gt/gt}* mouse showed that these mice also exhibited a decrease in the number of nephrons in the developing kidney [35] and cell cycle misregulation in the epithelium of the ocular lens [36]. Since the L27 and three PDZ domains of Dlgh-1 were left intact in the gene trap allele [34,37], it is possible that the fusion protein generated from this gene trap allele may retain some or acquire new activities of Dlgh-1 and, therefore, the phenotypes observed may not fully reflect the null phenotype. Consistent with this possibility, lacZ staining of *Dlgh-1^{gt/gt}* lenses and control *Dlgh-1^{+/+}* lenses showed similar staining patterns (Rivera and Griep, unpublished observations). Furthermore, two recent reports show that deletion of *Dlgh-1* in mice caused abnormalities in the ureteric smooth muscle [38] and absence of vagina and seminal vesicles [39]. Additionally, conditional deletion of *Dlgh-1* in the lens led to more severe phenotype than was observed in the lenses of the *Dlgh-1^{gt/gt}* mice including epithelial and fiber cell specific defects in cell adhesion and polarity [40].

In the present study, we generated mice carrying a germline null mutation in *Dlgh-1* by deleting one of the exons encoding the first PDZ domain and characterized the wide-ranging effects of this mutation on mouse embryogenesis. Loss of *Dlgh-1* not only recapitulated the craniofacial and kidney defects observed in the *Dlgh-1^{gt/gt}* mouse but also resulted in reduced ossification in the skull, maxilla, and middle ear, and shortening of the long bones. Furthermore, deletion of *Dlgh-1* resulted in eyelid closure and neural tube closure defects, and the misorientation of the stereociliary bundles of the cochlear hair cells, all of which suggest defects in PCP. Thus, our analysis identifies novel roles for *Dlgh-1* in mouse development, places Dlgh-1 in the group of factors that regulate PCP in the mouse, and provides new insight into the distinct *in vivo* requirements for this gene in vertebrates, as compared to invertebrates.

Results

Generation of *Dlgh-1* Null Mice

To generate *Dlgh-1* null mice, mice carrying a mutant allele of *Dlgh-1*, in which exon 8 and a neomycin resistance-cassette are flanked by loxP sites [40] (Fig. 1A), were mated to *EIII-Cre*

transgenic mice [41]. The *Dlgh-1* null allele was moved onto the FVB/NJ and C57BL/6J genetic backgrounds by backcrossing to either FVB/NJ or C57BL/6J mice for at least three generations before use. Mice heterozygous for the null allele were intercrossed to generate *Dlgh-1^{-/-}* mice and Southern blot analysis was used to confirm the genotype of the progeny (Fig. 1B).

To determine if the mutated *Dlgh-1* allele was indeed a null allele, Dlgh-1 protein levels in brain, heart, lung, kidney, skin, liver, and eyes of E18.5 *Dlgh-1^{+/+}*, *Dlgh-1^{+/-}*, and *Dlgh-1^{-/-}* mice were assessed by immunoblot analysis using an N-terminal specific anti-Dlgh-1 antibody. The Dlgh-1 protein levels were reduced by approximately 50% in the *Dlgh-1^{+/-}* mice compared to the *Dlgh-1^{+/+}* mice and Dlgh-1 protein was not detected in any of the tissues analyzed from the *Dlgh-1^{-/-}* mice or in mouse embryo fibroblasts (MEFs) derived from day E14.5 *Dlgh-1* null embryos (Fig. 1C). These results confirmed that the *Dlgh-1* mutant allele is a null allele.

Effect of Loss of *Dlgh-1* on Mouse Embryogenesis

It has been reported that mice homozygous for the *Dlgh-1^{gt}* allele die at or near the time of birth [12]. To determine if nullizygosity for *Dlgh-1* also would be lethal, we intercrossed *Dlgh-1^{+/-}* mice and examined litters for live *Dlgh-1^{-/-}* pups. Of the 47 pups genotyped, 10 were *Dlgh-1^{+/+}* (21%), 22 (47%) were *Dlgh-1^{+/-}*, and 15 (32%) were *Dlgh-1^{-/-}*. Of the 15 *Dlgh-1^{-/-}* pups, all of which exhibited severe craniofacial abnormalities, 13 were found dead on the day of birth and the remaining two died shortly after being found. These data indicate that loss of *Dlgh-1* confers perinatal lethality with 100% penetrance and support the hypothesis that *Dlgh-1* plays an important role in mouse development.

To understand the impact of the loss of *Dlgh-1* on mouse development, *Dlgh-1^{+/+}*, *Dlgh-1^{+/-}*, and *Dlgh-1^{-/-}* mice were collected at embryonic stages E11.5, E14.5, E16.5, and E18.5. *Dlgh-1^{-/-}* embryos were viable at all embryonic stages examined. However, at the gross level *Dlgh-1^{-/-}* embryos exhibited an abnormal head shape that included a shortened snout (Figs. 2A, H–I). *Dlgh-1^{-/-}* mice were smaller than their *Dlgh-1^{+/+}* counterparts. This reduction in size was apparent overtly (Fig. 2A) and in histological section by E14.5 (Figs. 2B, C). At the gross anatomic level, *Dlgh-1^{-/-}* mice also exhibited a secondary cleft-palate (Figs. 2D, E) that was consistent with the lack of a nasopharynx in these mutant animals observed in histological sections (Figs. 2F–I). All of these phenotypes of the *Dlgh-1^{-/-}* mice were observed with 100% penetrance on both the FVB/NJ and C57BL/6J genetic backgrounds and were similar to those observed in the *Dlgh-1^{gt/gt}* mice [34]. Additionally, the kidneys of the *Dlgh-1^{-/-}* mice were smaller in size and exhibited a reduced tubule to mesenchyme ratio (data not shown), consistent with a defect in branching morphogenesis, which was reported for the previously described *Dlgh-1* mutant mice [35,38]. Finally, defects in the ocular lens were also noted in the *Dlgh-1^{-/-}* mice (data not shown) as reported previously for the *Dlgh-1^{gt/gt}* mice [36] and mice in which *Dlgh-1* was specifically deleted in the lens [40]. Together, these data show that *Dlgh-1* is required for mouse survival, likely in part through its contribution to palate formation, and for multiple aspects of mouse development.

Effect of Loss of *Dlgh-1* on Eyelid and Neural Tube Closure

The cleft palate and reduced size of the *Dlgh-1^{-/-}* mice (Fig. 2) were observed on both the FVB/NJ or C57BL/6J backgrounds. However, some defects were noted exclusively on the C57BL/6J background. First, eyelid closure defects were apparent in 100% of

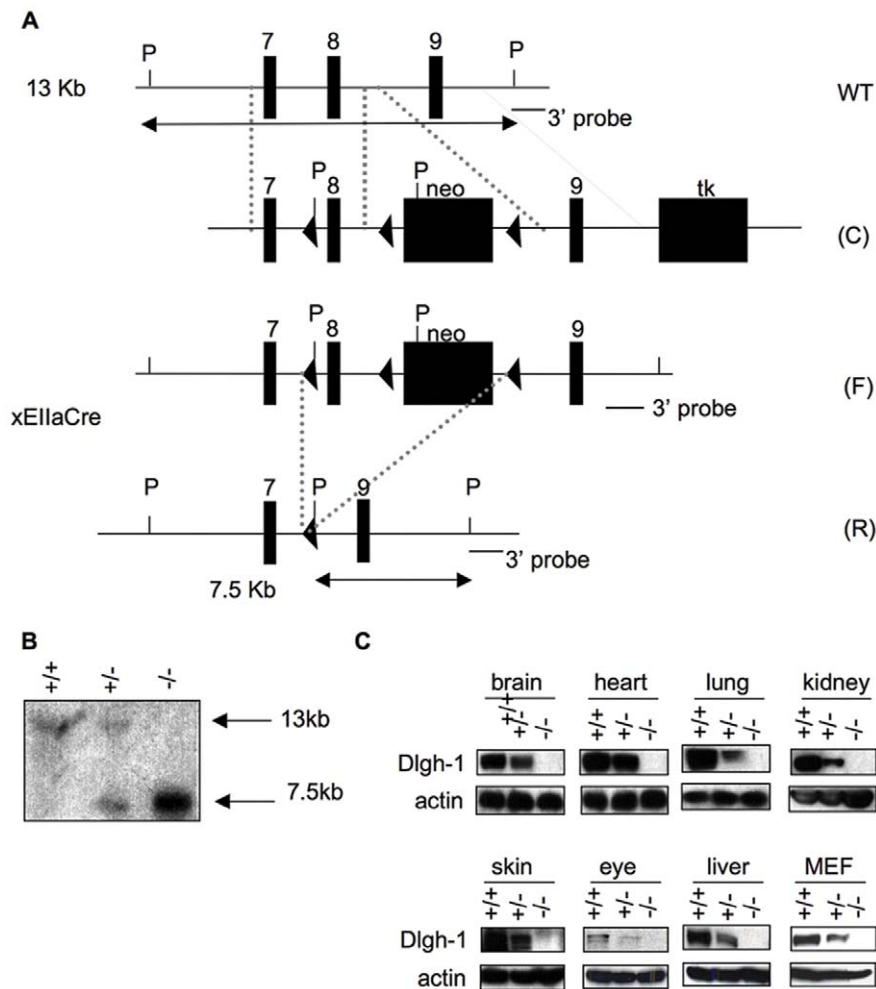


Figure 1. Generation of *Dlgh-1* null mice. (A) Schematic representation of the targeting of the *Dlgh-1* allele. WT, wild-type allele; C, construct, plasmid containing loxP sites flanking exon 8 of *Dlgh-1* and neo cassette, and the TK cassette; F, the floxed allele, containing lox P sites flanking *Dlgh-1*'s exon 8 and the neo cassette; R, recombined allele, desired recombination event lacking exon 8 and neo. Abbreviations: 7, exon 7; 8, exon 8; 9, exon 9; P, *PstI*; triangles, lox P sequences; neo, neomycin; TK, thymidine kinase. 3' probe for Southern blot analysis is denoted by black bars. Fragments expected from *PstI* digestion and 3' probe hybridization are depicted by double-headed lines. (B) Southern blot analysis of *PstI* digested genomic DNA isolated from mice that were WT (+/+), heterozygote (+/-), or null (-/-) for the *Dlgh-1* allele. Sizes of hybridizing bands are shown in kb. (C) Western blot analysis of *Dlgh-1* protein levels. Protein lysates of brain, heart, lung, kidney, skin, eye, liver, and mouse embryo fibroblasts (MEF) from *Dlgh-1* wild type (+/+), heterozygote (+/-), or null (-/-) mice were resolved by SDS-PAGE and immunoblotted with an anti-*Dlgh-1* antibody, as described in Materials and Methods. Membranes were reprobed with an anti- β -actin antibody as a loading control. doi:10.1371/journal.pone.0054410.g001

C57BL/6J *Dlgh-1*^{-/-} mice at E18.5 (Fig. 3). The severity of this phenotype varied. In some cases the epidermis had extended and fused; however, the dermis had not filled in (Fig. 3E). In other cases, the epidermis had failed to extend, leading to a complete failure of eyelid closure (Fig. 3F). To determine if the effect of *Dlgh-1* deficiency on eyelid closure may be a direct effect, head sections from *Dlgh-1*^{+/+} and *Dlgh-1*^{-/-} mice were subjected to double immunofluorescence experiments using anti-*Dlgh-1* and anti-Vangl2 antibodies (Fig. 4). Staining for *Dlgh-1* was observed in the *Dlgh-1*^{+/+} eyelid epithelium (Fig. 4A, B) but was absent in the *Dlgh-1*^{-/-} eyelid (Fig. 4D, E), suggesting that the open eyelid defect may be a direct result of loss of *Dlgh-1* function.

Interestingly, the failure of eyelid closure is also noted in the *circletail* (*Crc/Crc*) mouse, in which a defective Scrib protein lacking the C-terminal two PDZ domains is expressed [42], and in the *looptail* (*Vangl2*^{Lp/Lp}) mouse, in which a defective Vangl2 protein carrying an amino acid substitution mutation (S464N) is expressed [43,44]. The Vangl2 protein is normally expressed in the eyelid

epithelium [43,44,45] and is primarily localized to the plasma membrane [45]. However, the mutant Vangl2 protein in *Vangl2*^{Lp/Lp} mice fails to localize to the membrane; rather it is cytoplasmic [45]. Immunofluorescent staining of eyelids from *Dlgh-1*^{+/+} mice showed that Vangl2 was tightly localized to the membranes in the eyelid epithelium (arrow, Fig. 4A, C) where there was overlap with *Dlgh-1* staining. In contrast, Vangl2 was cytoplasmic in the eyelid of the *Dlgh-1*^{-/-} mice (Fig. 4D, F). Thus, the correct subcellular localization of Vangl2 in the eyelid epithelium depends on *Dlgh-1*.

Vangl2^{Lp/Lp} and *Crc/Crc* mice also exhibit craniorachischisis [42,44,46], a severe neural tube closure defect in which the neural tube is open from the midbrain-hindbrain boundary to the tail. This same neural tube defect was observed in C57BL/6J *Dlgh-1*^{-/-} mice at both E16.5 (Figs. 5C, D) and E18.5 (not shown). Unlike the open eyelid phenotype, however, craniorachischisis occurred with low penetrance; only 6.7% (2 out of 30) of the C57BL/6J *Dlgh-1* null mice displayed this defect. *Dlgh-1*^{-/-} mice that exhibited craniorachischisis also exhibited gastroschisis, an exter-

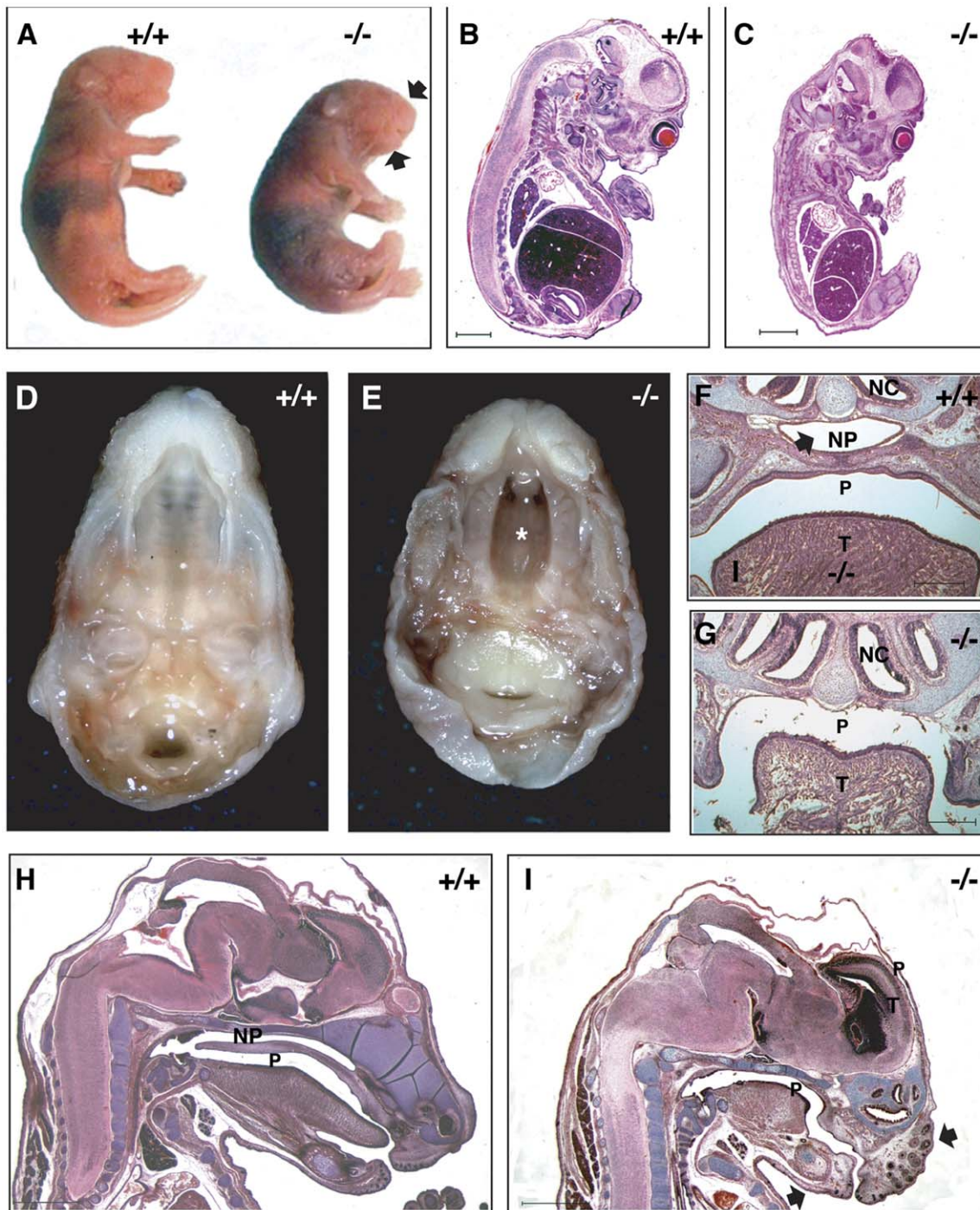


Figure 2. Phenotype of *Dlgh-1*^{-/-} mice. (A) Newborn *Dlgh-1*^{-/-} mice are smaller than their *Dlgh-1*^{+/+} counterparts and have a shortened snout and mandible (arrows). (B–C) Hematoxylin and eosin stained paraffin sections of FVB/NJ E14.5 *Dlgh-1*^{+/+} (B) and *Dlgh-1*^{-/-} (C) mice. At this developmental stage, the reduced size of the *Dlgh-1*^{-/-} is noticeable. (D–E). Dissected heads of *Dlgh-1*^{+/+} and *Dlgh-1*^{-/-} C57BL/6J E18.5 embryos showing the cleft palate (asterisk*) in *Dlgh-1*^{-/-} mice. (F–G) Frontal sections of *Dlgh-1*^{+/+} (F) and *Dlgh-1*^{-/-} (G) E18.5 embryos on the C57BL/6J background showing the absence of the nasopharyngeal passage (NP, arrow in F). (H–I) Sagittal H&E stained sections of E18.5 *Dlgh-1*^{+/+} (H) and *Dlgh-1*^{-/-} (I) embryos on the FVB/NJ background showing the dome-shaped head of *Dlgh-1*^{-/-} mice, the absence of the nasopharyngeal passage (NP), and the shortened snout and mandible (arrows). NC, nasal cavity; NP, nasopharyngeal passage; P, pharynx; T, tongue. Scale bar = 250 μm. doi:10.1371/journal.pone.0054410.g002

nalization of the gut (Fig. 5A, C). Closure of the eyelid and neural

tube closure exhibited in the *Dlgh-1*^{-/-} mice suggest a new role for *Dlgh-1* in the mouse in the regulation of convergent extension.

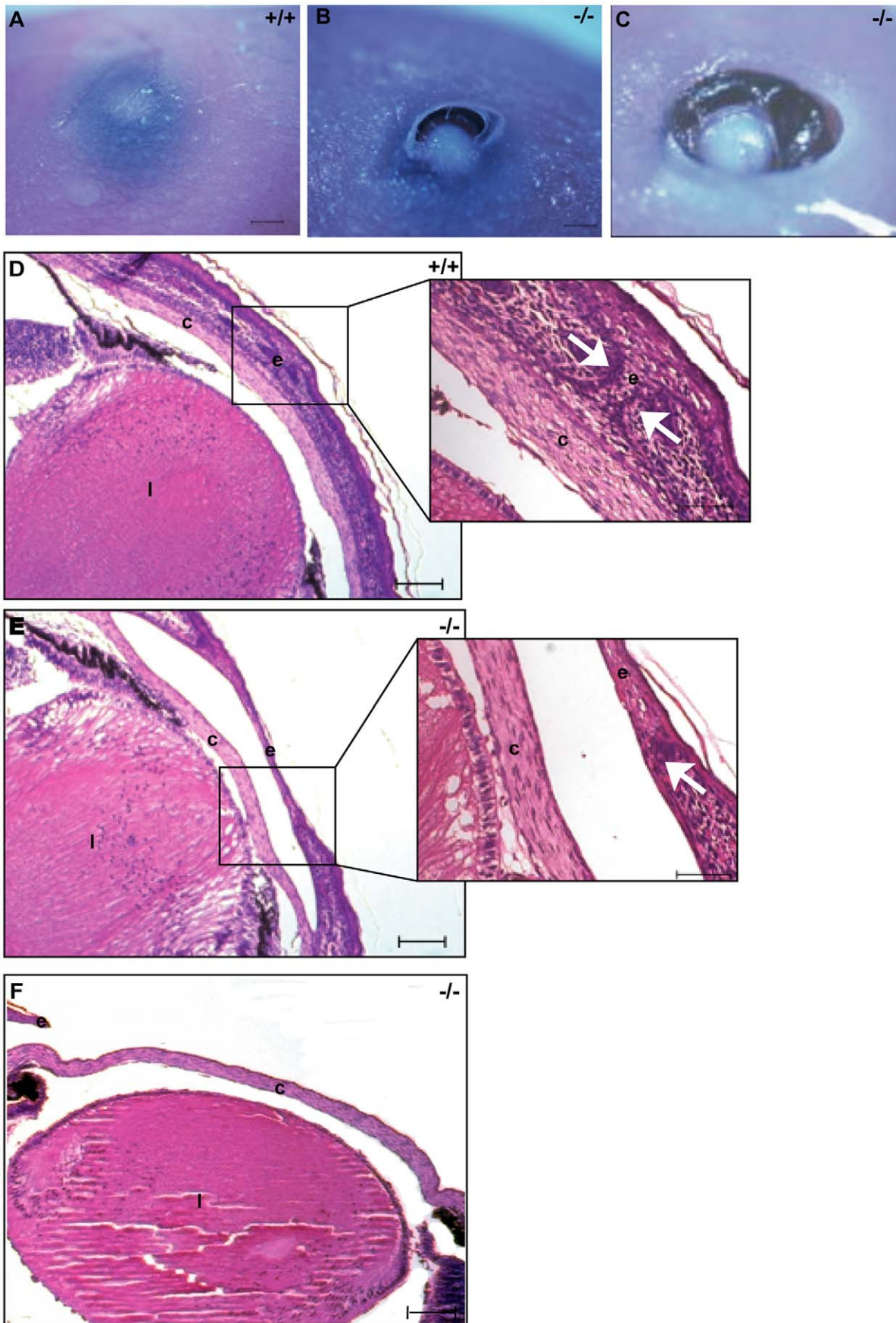


Figure 3. *Dlgh-1*^{-/-} mice display defects in eyelid closure. E18.5 *Dlgh-1*^{+/+} and *Dlgh-1*^{-/-} mice on the C57BL/6 background were collected and analyzed for the presence of closed eyelids. *Dlgh-1*^{+/+} mice (A) form closed eyelids while *Dlgh-1*^{-/-} (B, C) littermates show defects in eyelid closure. (D–F) Hematoxylin and eosin staining of histological sections collected from E18.5 mice show completely closed eyelids in *Dlgh-1*^{+/+} mice (D) whereas eyelids in *Dlgh-1*^{-/-} mice were only partially closed (E) or completely open (F). Insets show a higher magnification of the eyelids. Arrows show the position of the tips of the dermis in *Dlgh-1*^{+/+} (D) and *Dlgh-1*^{-/-} (E) embryos, which failed to extend fully in the *Dlgh-1*^{-/-} eye. Scale bar = 250 μm and 150 μm for insets. c, cornea; e, eyelids; l, lens.
doi:10.1371/journal.pone.0054410.g003

Effect of the Loss of *Dlgh-1* on Cochlear Hair Cell Stereociliary Bundle Orientation

Recent studies in vertebrates have shown that convergent extension is regulated, at least in part, by a group of proteins that are involved in planar cell polarity (PCP) in *Drosophila* [3]. PCP refers to the polarization of cells within the plane of a cell sheet. In *Drosophila*, PCP regulates wing hair, body bristle, and eye ommatidial cluster orientation. In mammals, the uniform orientation of stereociliary bundles of the hair cells within the cochlea represents a distinctive example of PCP. In *Vangl2*^{Lp/Lp} mice, the stereociliary bundles in the inner (IHC) and outer (OHC) hair cell layers are misoriented [4]. Similarly, in *Crc/Crc* mice the stereociliary hair bundles in the second and third row of OHCs are misoriented [4]. Together, these data identify a role for *Vangl2* and *Scrib* in the regulation of the PCP pathway in vertebrates.

Because *dlg* and *scrib* are known to interact in *Drosophila* [2] and because the open eyelid, neural tube, and gut phenotypes of the

Dlgh-1^{-/-} embryos (Fig. 4) resemble that of *Crc/Crc* mutant mice [42], we asked if stereociliary bundle orientation was affected in the *Dlgh-1* null mice. Cochlear sensory epithelia (organs of Corti) from E18.5 *Dlgh-1*^{+/+} and *Dlgh-1*^{-/-} embryos were stained with phalloidin to label hair cell stereocilia, a structure rich in filamentous actin, and the specimens analyzed by confocal microscopy. Normally, the stereociliary bundles are arranged uniformly around the primary cilia and oriented toward the outer edge of the organ. The IHC bundles are arranged in a curved shape while the OHC bundles are arranged in a v-shape [48]. The stereociliary bundles in the IHC row of the *Dlgh-1*^{-/-} mice were uniformly polarized, as in the *Dlgh-1*^{+/+} mice (Fig. 6A, B). The stereociliary bundles in all three rows of OHCs of the *Dlgh-1*^{+/+} mice were uniformly oriented (Fig. 6A). However, many stereociliary bundles in the third row of OHCs in the *Dlgh-1*^{-/-} cochleae were misoriented (Fig. 6B, arrows). Occasionally, stereociliary bundles in the second OHC layer were also misoriented (Fig. 6B). The angle of orientation of individual

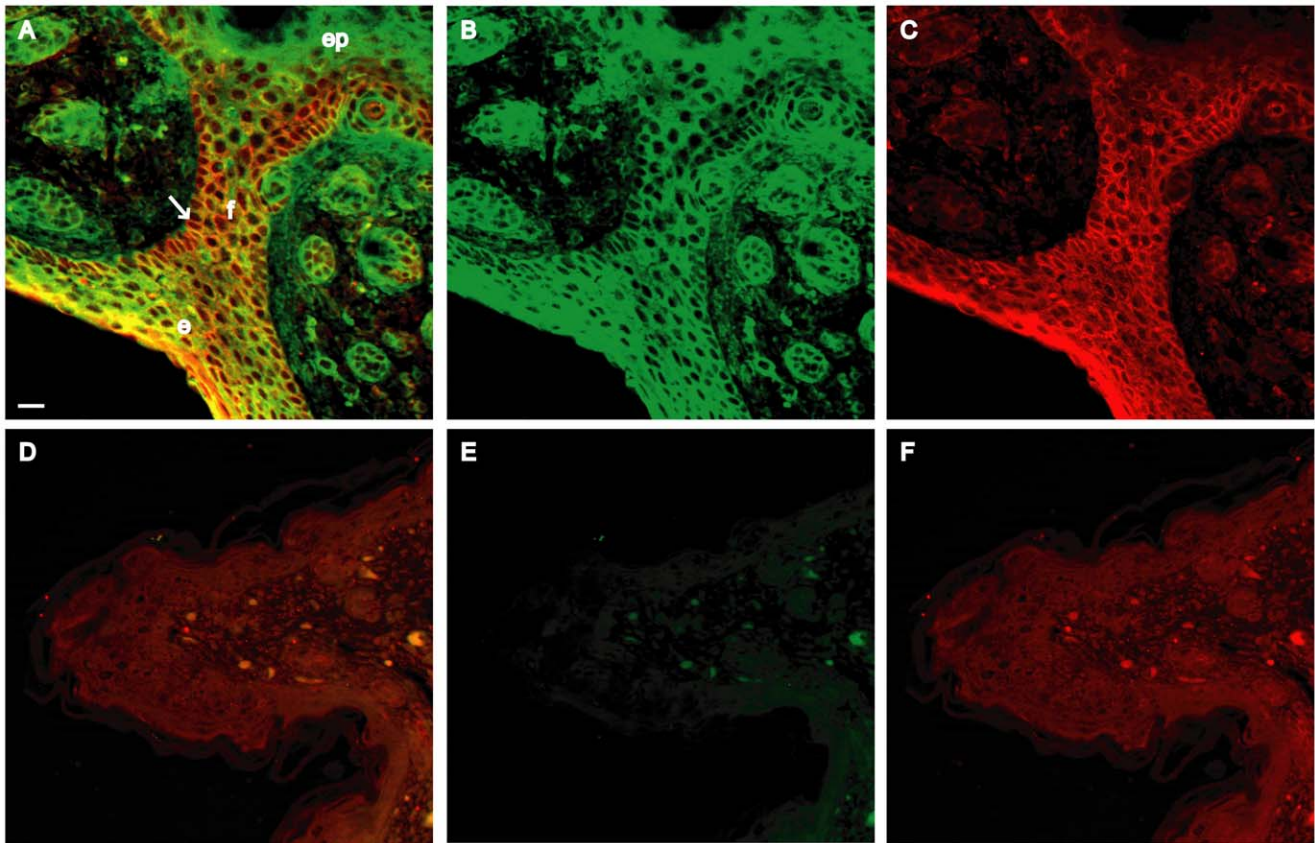


Figure 4. Expression of *Dlgh-1* and *Vangl2* proteins in the eyelid of *Dlgh-1*^{+/+} and *Dlgh-1*^{-/-} mice. Sections of sagittally oriented, paraffin embedded heads from newborn *Dlgh-1*^{+/+} (A–C) and *Dlgh-1*^{-/-} (D–F) mice on the C57BL/6J background were subjected to double immunofluorescence analysis with anti-*Dlgh-1* (green) and anti-*Vangl2* (red) antibodies. Shown are representative merged and unmerged images of the staining in the eyelid of *Dlgh-1*^{+/+} (A–C) and *Dlgh-1*^{-/-} (D–F) eyelids. *Dlgh-1* (A, B) and *Vangl2* (A, C) localized to the membranes of the epithelium (arrow in A) including the site of eyelid fusion, in *Dlgh-1*^{+/+} mice. Staining for *Dlgh-1* was absent in eyelid of the *Dlgh-1*^{-/-} mice (E) and *Vangl2* accumulated in the cytoplasm rather than in the membrane (D, F). e, epithelium; ep, epidermis; f, eyelid fusion. Scale bar = 50 μm.
doi:10.1371/journal.pone.0054410.g004

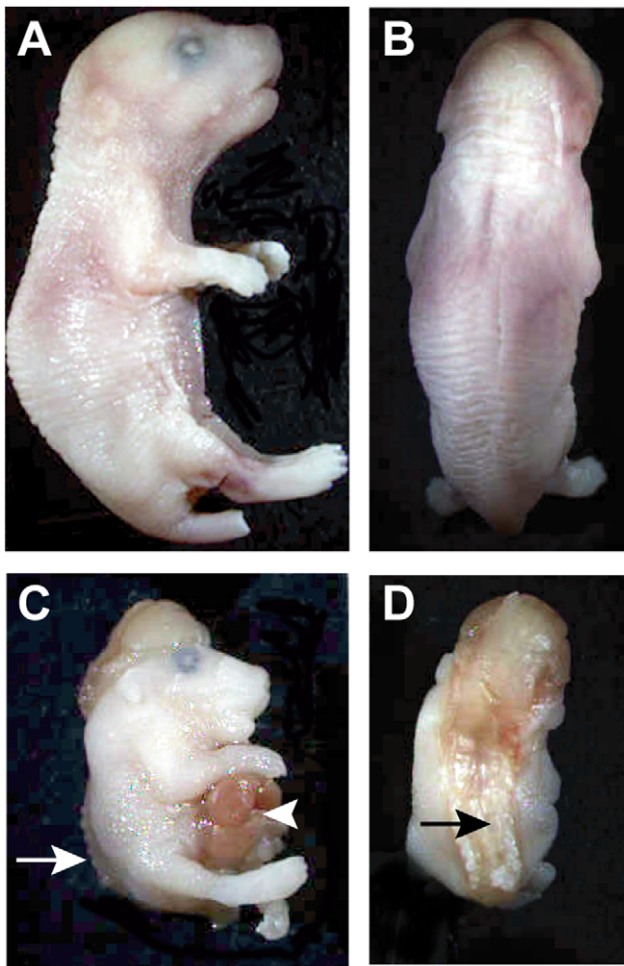


Figure 5. A fraction of *Dlgh-1*^{-/-} mice display defects in neural tube closure. E16.5 *Dlgh-1*^{+/+} and *Dlgh-1*^{-/-} embryos on the C57BL/6J background were collected, examined for overt defects, and photographed under a dissecting microscope. Profile (A) and dorsal (B) views of an E16.5 *Dlgh-1*^{+/+} embryo. Profile (C) and dorsal (D) views of an E16.5 *Dlgh-1*^{-/-} embryo. In addition to craniorachischisis (C, D arrows), the *Dlgh-1*^{-/-} embryo exhibits gastroschisis (C, arrowhead) and a rightward kink to the body axis (D).
doi:10.1371/journal.pone.0054410.g005

stereociliary bundles in the OHC3 layer relative to the neural-abneural axis in *Dlgh-1*^{+/+} and *Dlgh-1*^{-/-} cochlea were measured and the degrees of deviation from this axis calculated (Fig. 6C). The average degrees of deviation for bundles in the *Dlgh-1*^{-/-} mice (33.7±1.87 degrees) was significantly higher ($p = 1.5 \times 10^{-9}$) than in the *Dlgh-1*^{+/+} mice (17.3±0.87 degrees). To determine if the effect of *Dlgh-1* deficiency on the cochlea might be a direct effect, head sections from day E15.5 *Dlgh-1*^{+/+} embryos were immunostained with an anti-Dlgh-1 antibody (Fig. 6D). Immunoreactivity was observed in the epithelial cells of the duct, which give rise to the sensory cells, and cartilage within the cochlea, indicating the presence of Dlgh-1 protein in these structures. To further determine if the effect of Dlgh-1 deficiency on hair cell orientation might be a direct effect, cochlear explants from P2 control mice were subjected to immunofluorescence for Dlgh-1. Immunoreactivity was observed in the basal-lateral membrane domain of the outer hair cells (Fig. 6F, arrows). The expression of Dlgh-1 in tissues such as the eyelid and hair cells, which show defects in the *Dlgh-1*^{-/-} mouse, together with the

open eyelid, mislocalization of PCP protein Vangl2 in the open eyelid, craniorachischisis, and misorientation of cochlear stereociliary in the *Dlgh-1*^{-/-} mice (Figs. 3, 4, 5, 6) suggest a role for *Dlgh-1* in the regulation of PCP in the mouse.

Effect of the Loss of *Dlgh-1* in Skeletogenesis

The *Dlgh-1*^{gt/gt} mice exhibited a cleft palate and a hypotrophic mandible [34], suggesting that *Dlgh-1* may be required for the formation of at least certain craniofacial bones. To test this hypothesis, the skeletal frames of E18.5 *Dlgh-1*^{+/+}, *Dlgh-1*^{+/-}, and *Dlgh-1*^{-/-} mice on both the FVB/NJ and C57BL/6J background were stained with alizarin red and alcian blue to visualize bone and cartilage, respectively. *Dlgh-1*^{-/-} mice on both the FVB/NJ (Fig. 7) and C57BL/6J (not shown) genetic backgrounds had shorter mandibles (MA) and maxillas (MX), which was consistent with the short snout phenotype. However, uniquely on the FVB/NJ background, *Dlgh-1*^{-/-} mice also showed additional skeletal defects. *Dlgh-1*^{-/-} embryos exhibited reduced ossification of multiple craniofacial structures including the nasal bone (N), the retrotympenic process (RTP), and the tympanic bone (T) (Figs. 7A, C). Interestingly, the developing calvarium was also affected as the ossification of the frontal bone (F) and the parietal bone (P) were reduced or absent in the *Dlgh-1*^{-/-} mice (Fig. 7C). Furthermore, the parietal bone was absent in one *Dlgh-1*^{+/-} specimen on the FVB/NJ background, suggesting a dosage-dependent effect of *Dlgh-1* on calvarium development (Fig. 7B).

The skeletal defects in the *Dlgh-1*^{-/-} mice on the FVB/NJ background extended to a reduction in the ossification of the ribs, as well as the second, third, and fourth sternbrae (S) (Fig. 7E). The long bones of the fore- and hindlimbs were also shortened by approximately 20% and 18%, respectively, in the *Dlgh-1*^{-/-} mice when compared to their *Dlgh-1*^{+/+} counterparts (Figs. 7F, G). Calcification in the phalanges, while apparent in the limbs of the *Dlgh-1*^{+/+} mice, was absent in the limbs of the *Dlgh-1*^{-/-} mice (Figs. 6F, G, arrow). Taken together, these results suggest that *Dlgh-1* is required for proper skeletogenesis of craniofacial, axial and long bones. Furthermore, as the calvarium forms through intramembranous bone formation whereas the other craniofacial bones and the axial bones form through endochondral ossification [49], these data show that both forms of bone development are affected when *Dlgh-1* is ablated in the mouse.

Discussion

The MAGUK protein Dlgh-1, which is highly conserved cross-species, has emerged as an important factor in the regulation of cell-cell adhesion, apical-basal polarity, and cell proliferation in *Drosophila* [1,2]. The regulation of these cellular aspects is critical for the establishment of specialized organs during embryogenesis. In the current study, we assess the role of *Dlgh-1* in mouse embryogenesis (see Table 1 for a summary of phenotypes). We provide evidence that loss of *Dlgh-1* affects PCP during mouse embryogenesis. We further provide evidence that loss of *Dlgh-1* causes defects in skeletal structures arising through both endochondral and intramembranous ossification. These findings demonstrate newly discovered roles for *Dlgh-1* in vertebrate development and suggest that the *Dlgh-1*^{-/-} mouse may serve as an animal model to study major congenital birth defects in humans such as defects in neural tube closure and skeletal malformations.

Role of *Dlgh-1* in Mouse Organogenesis

The results presented in this study suggest that *Dlgh-1* plays a vital role during mouse organogenesis. Defects in the mandible,

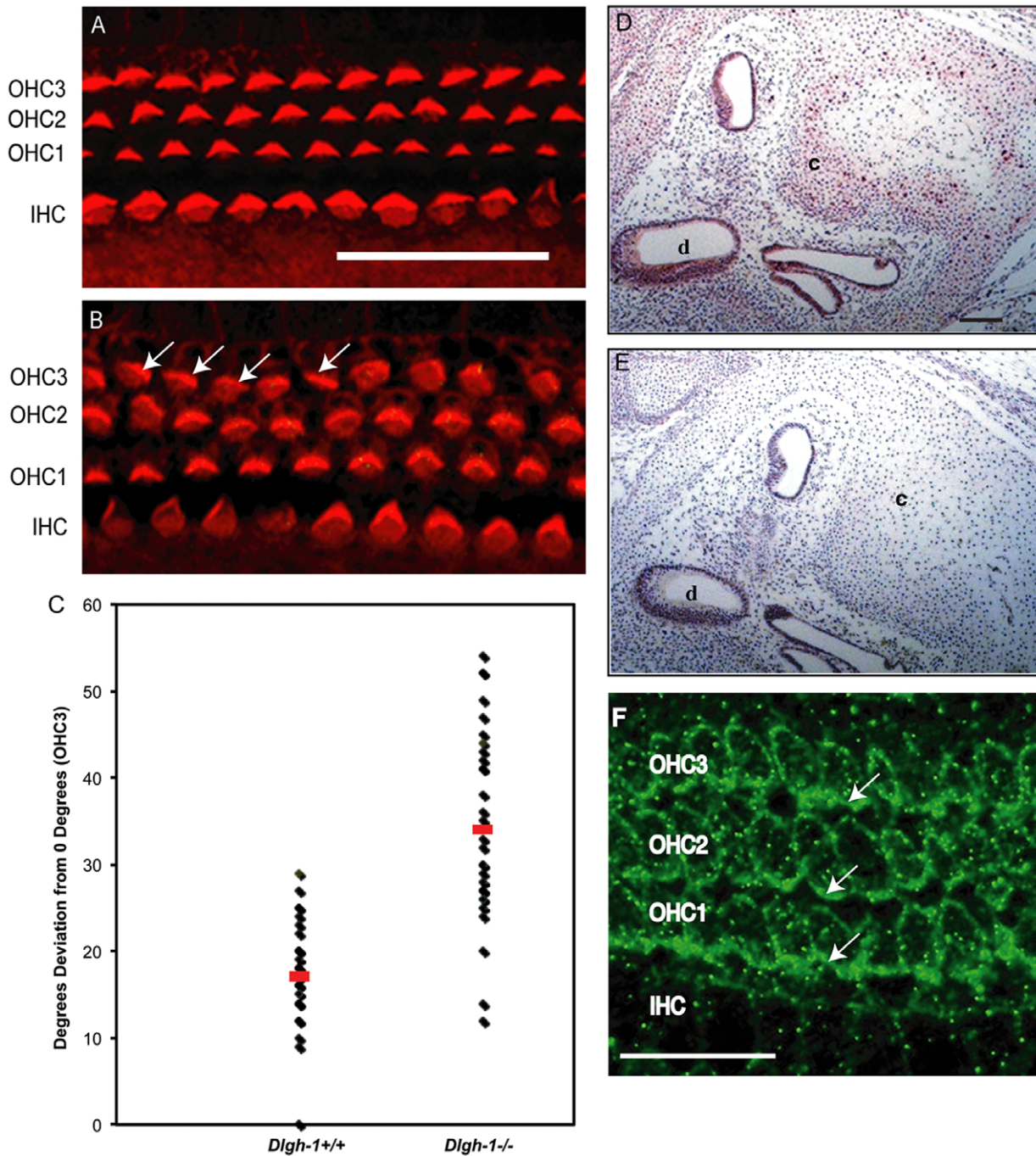


Figure 6. *Dlgh-1*^{-/-} mice display defects in outer cell hair polarity. (A, B) Representative images of the OHC and IHC layers in the cochlea of *Dlgh-1*^{+/+} and *Dlgh-1*^{-/-} mice. The organ of Corti was isolated from the cochleae of E18.5 *Dlgh-1*^{+/+} (A) and *Dlgh-1*^{-/-} (B) embryos, stained with phalloidin to visualize the actin bundles of the inner and outer hair cells, and viewed by confocal microscopy. Arrows indicate cells with misoriented stereociliary bundles in OHC3 row of the *Dlgh-1*^{-/-} mice. (C) Measurement of misorientation of stereociliary bundles in OHC3 layer of *Dlgh-1*^{+/+} and *Dlgh-1*^{-/-} mice. The angle of stereociliary bundles in OHC3 of *Dlgh-1*^{+/+} and *Dlgh-1*^{-/-} mice was measured in reference to a line parallel to the neural-abneural axis and perpendicular to the plane of the pillar cells. Plotted is the deviation in degrees from the neural-abneural axis for each OHC3 bundle measured in (4 cochleae from 3 mice of each genotype, 36 cells for *Dlgh-1*^{+/+} and 33 cells for *Dlgh-1*^{-/-} mice). No deviation from the neural-abneural axis was assigned a value of 0°. The average angle deviation from 0° for OHC3 bundles in *Dlgh-1*^{-/-} cochlea (33.7°±1.869, red bar) was significantly higher ($p=1.5\times 10^{-9}$) than that of the *Dlgh-1*^{+/+} (17.3°±0.869, red bar). (D, E) Immunohistochemical detection of *Dlgh-1* protein in the cochlea of E15.5 mouse embryos. Transverse sections of paraffin embedded heads from control *Dlgh-1*^{+/+} mice were subjected to immunohistochemistry using (D) an anti-*Dlgh-1* specific antibody and alkaline phosphatase detection or (E) no primary antibody. The pink color in the epithelium of the cochlear duct and cartilage in (D) is indicative of the presence of *Dlgh-1* protein in these structures. (F) Immunofluorescent detection of *Dlgh-1* protein in the cochlear hair cells of P2 mice control. Fixed cochlear explants from *Dlgh-1*^{+/+} mice were subjected to immunofluorescence using an anti-*Dlgh-1* (green) antibody. Arrows show concentration of *Dlgh-1* on the basal-lateral membranes of the OHC cells. IHC, inner hair cells, OHC1, 2, 3, outer hair cell rows 1, 2, and 3. c, cartilage in cochlea, d, cochlear duct. Scale bar = 50 μm.

doi:10.1371/journal.pone.0054410.g006

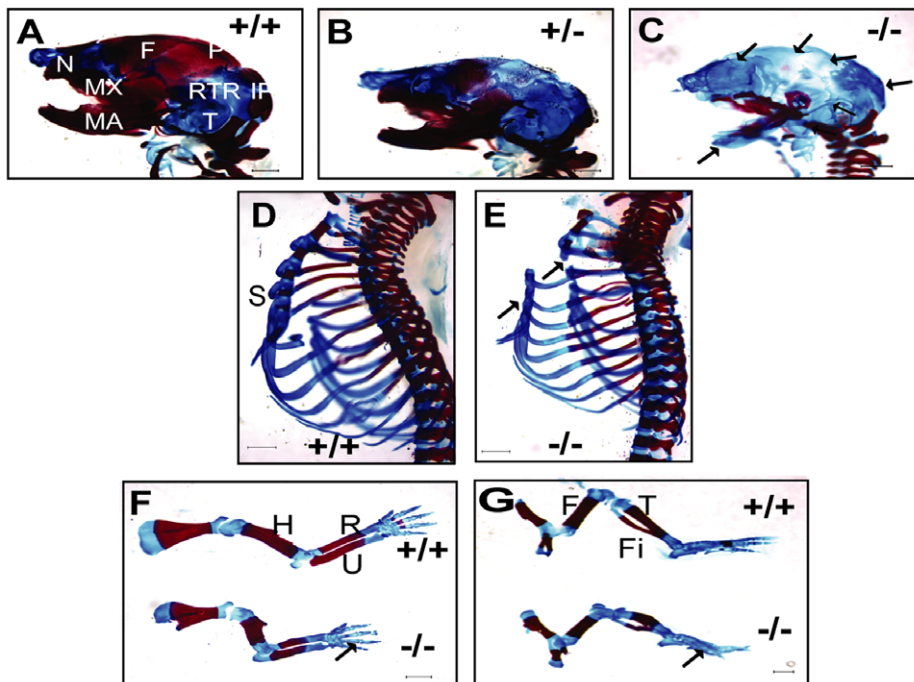


Figure 7. *Dlgh-1*^{-/-} mice display defects in skeletogenesis. Eviscerated carcasses of E18.5 *Dlgh-1*^{+/+}, *Dlgh-1*^{+/-}, and *Dlgh-1*^{-/-} mice on the FVB/NJ background were prepared and stained for cartilage and bone with alcian blue and alizarin red, respectively. Craniofacial skeleton in (A) *Dlgh-1*^{+/+}, (B) *Dlgh-1*^{+/-}, and (C) *Dlgh-1*^{-/-} mice. Arrows show loss of bone formation in *Dlgh-1*^{+/-} and *Dlgh-1*^{-/-} mice. F, frontal bone; IP, intraparietal bone; P, parietal bone; N, nasal; Ro, rostral bone; RTP, retrotemporal process; T, temporal bone. (D–G) Axial structures of *Dlgh-1*^{+/+} (D) and *Dlgh-1*^{-/-} mice (E). Forelimb (F) and hindlimb (G) structures. Arrows show the absence of bone formation in *Dlgh-1*^{-/-} mice. S, sternbrae; H, humerus; R, radius; U, ulna; F, femur; Fi, fibula; T, tibia. Scale bar in A–E = 1000 μm, in F = 650 μm and in G = 500 μm.
doi:10.1371/journal.pone.0054410.g007

the kidneys, and the lens have been previously described in the *Dlgh-1*^{gt/gt} mice [34,35,36]. The formation of these structures and organs was likewise affected in our *Dlgh-1* null mice (Fig. 2 and data not shown). More recently, novel defects in the ureteric smooth muscle and the urogenital tract have been observed in *Dlgh-1*^{-/-} mice [38,39]. In the present study, we provide evidence for *Dlgh-1* playing a role in the skeletogenesis of trunk and limb structures, in neural tube and eyelid closure, and in the

organization of the stereociliary bundles in the cochlea. These latter phenotypes were not reported previously in mice carrying the gene trap insertion in *Dlgh-1* [34] and we have not observed open eyelids or open neural tubes in C57BL/6 *Dlgh-1*^{gt/gt} mice in our laboratory (M.M. Nguyen, C. Rivera, and A.E. Griep, unpublished observations). As the N-terminal portion of *Dlgh-1* including the L27 and three PDZ domains are intact in the *Dlgh-1*^{gt} fusion protein [34,37], it is likely that the function of one or more of these protein-protein interaction domains is required for *Dlgh-1*'s role in the novel phenotypes we have observed.

Table 1. Summary of Phenotypes in *Dlgh-1* Null Mice.

Defect	Mouse Strain	Penetrance	Reported in <i>Dlgh</i> ^{gt} mice
Perinatal lethality	Both	100%	Yes
Cleft palate	Both	100%	Yes
Shortened snout	Both	100%	Yes
Reduced size	Both	100%	Yes
Eyelid closure	C57BL/6J	100% ^a	No
Neural tube closure	C57BL/6J	6.7%	No
Cochlear hair cells	C57BL/6J	100%	No
Skeletal ^b	FVB/NJ	100%	No

^aEyelid closure defects were observed in 100% of *Dlgh-1*^{-/-} mice on the C57BL/6J background. However, the severity of the phenotype varied from animal to animal.

^bDefects in bone formation were observed throughout the head, trunk and limbs of the *Dlgh-1*^{-/-} embryos on the FVB/NJ background.

doi:10.1371/journal.pone.0054410.t001

Role of *Dlgh-1* in Planar Cell Polarity

Planar cell polarity is the mechanism through which the orientation of cells is coordinated within the plane of a cell sheet. In vertebrates, PCP has been suggested to be required for several developmental processes that involve convergent extension, such as lengthening of the body axis, eyelid closure, neural tube closure, branching morphogenesis in the kidney and lung, and the stereociliary cell hair bundle orientation in cochlea [3]. *Dlgh-1*^{-/-} mice, with variable penetrance, exhibited a reduced body length to width ratio, open eyelids (Fig. 3), craniorachischisis (Fig. 5), and misorientation of stereocilia in the third row of cochlear OHCs (Fig. 6). Moreover, *Dlgh-1* is expressed in the eyelid epithelium (Fig. 4A, B) and cochlear hair cells (Fig. 6F) and *Dlgh-1* deficiency led to mislocalization of the core PCP protein, Vangl2, in the mutant eyelid (Fig. 4D, F). Thus, this study provides the first evidence in support of a role for *Dlgh-1* in the regulation of PCP in the mouse *in vivo*.

Although much remains to be learned about the molecular and genetic mechanisms regulating PCP, from studies in the *Drosophila* eye and wing, factors including Frizzled (Fz), Dishevelled (Dsh),

Strabismus/Van Gogh (stbm/Vang), and Starry night/Flamingo (Stan/Fmi) are thought to mediate PCP through non-canonical Wnt signaling [3]. This pathway appears to be highly conserved in vertebrates. Wnt signaling has been shown to be required for mediating the organization of cochlear OHCs into their distinctive unidirectional orientation during development [48,50]. *Fz3*^{-/-}; *Fz6*^{-/-}, *Dvl1*^{-/-}; *Dvl2*^{-/-}, and *Lp/Lp* mice show reduced body length to width ratio, craniorachischisis, failure of eyelid closure, and misorientation of stereociliary bundles at the apices of sensory hair cells [4,42,51,52,53]. Additionally, this small group of factors in vertebrates includes Celsr1 [54], a protocadherin and homolog of *Stan/Fmi*, and PTK 7, a protein tyrosine kinase [55].

Interestingly, Fz3, Fz6, and Vangl2 contain C-terminal PDZ binding motifs whereas Dvl1 and Dvl2 are PDZ domain proteins, suggesting that PDZ domain proteins and their ligands interact to play a major role in PCP. *Dvl2* genetically interacts with *Vangl2* and *Vangl2* is required for the proper membrane localization of Dvl2 in the cochlear hair cells [52]. *Vangl2* interacts with Fz3 and is required for targeting of Fz3 to the membrane of the cochlear hair cells [56]. It has recently been shown that these core PCP proteins also interact with other PDZ proteins in vertebrate systems. Fz4 and Fz7 have been shown to interact with the MAGUK protein, MAGI-3, through the PDZ binding motif of Fz and the first PDZ domain of MAGI-3 *in vitro* and in epithelial cells [57] and *Dlgh-1* has been shown to interact through its PDZ domain with the C-terminal PDZ binding motif in Fz1, Fz4, and Fz7 at least in yeast two hybrid experiments [58,59]. Mice defective for the PDZ protein *Scrib* (*Crc/crc* mice) exhibit the same phenotypes as mouse *Fz*, *Dvl*, and *Vangl2* mutants. *Scrib* been shown to genetically interact with *Vangl2* to modulate PCP in the cochlea [4] and *Scrib* binds to *Vangl2* [56]. In this study, we have shown that the phenotype of *Dlgh-1* null mice bears many similarities to the phenotypes of PCP mutant mice. Furthermore, we have shown that *Dlgh-1* is expressed in the eyelid epithelium (Fig. 4A, B) and the outer hair cells of the cochlea (Fig. 6F) and is required for correct subcellular localization of *Vangl2* in the eyelid (Fig. 4D, F). Therefore, we suggest that *Dlgh-1* also is a member of this group of factors involved in the regulation of PCP in the mouse, which is has very recently been shown to include another mouse *Dlg*, *Dlg-3* [60]. The role for *Dlgh-1* in PCP in properly localizing *Vangl2* to the membrane may be a critical function for PCP as *Vangl2* has been shown to be required for proper localization of Fz3 [56] and Dvl2 [61,62].

We observed differences in the phenotypes of *Dlgh-1*^{-/-} embryos depending on the genetic background. On the C57BL/6J background, eyelid closure defects were present in 100% and craniorachischisis was present in 6.7% of *Dlgh-1*^{-/-} embryos (Figs. 3, 5). Neither of these phenotypes was observed in *Dlgh-1*^{-/-} embryos on the FVB/NJ background. The low penetrance of craniorachischisis in *Dlgh-1*^{-/-} embryos on the C57BL/6J background is similar to observations of low penetrance of craniorachischisis in *Dvl1*^{-/-}; *Dvl2*^{-/-} mice on the C57BL/6J background. By contrast the penetrance of craniorachischisis is high on the 129 background [52]. The observation that the penetrance of some phenotypes associated with PCP is dependent on mouse genetic background suggests either that there are additional genetic modulators of PCP that have yet to be identified or that polymorphisms in one or more of the already identified genes on these different genetic backgrounds influences PCP.

Role of *Dlgh-1* in Skeletogenesis

The cleft palate and hypotrophic mandible in the *Dlgh-1*^{gt/gt} mice indicated that this PDZ domain protein might be important in the development of craniofacial skeletal structures [34]. The

Dlgh-1^{-/-} mice not only recapitulated the craniofacial defects observed in the *Dlgh-1*^{gt/gt} mice, but also displayed reduced ossification of the maxilla, middle ear, frontal, and parietal bones and overall reduced size of the skeleton (Fig. 7).

One mechanism through which loss of *Dlgh-1* may affect craniofacial development is through disruption of WNT/PCP signaling [63]. Recently, it has been shown that certain core Wnt/PCP proteins are expressed in cranial neural crest (CNC) cells [64,65], which give rise to most of the skeletal structures of the head and neck, and these core PCP proteins are required for CNC migration [66]. As noted above, *Dlgh-1* has been shown to bind to several Fz receptors, including those commonly associated with Wnt/PCP signaling [58,59]. Likewise, *Wnt5a*, which has been suggested to be a regulator of Wnt/PCP signaling in the mouse [50], is expressed in outgrowing regions of the facial primordia and *Wnt5a* mutant mice display abnormally shaped head and shortened snout and mandible [67]. Finally, *Wnt5a* deficiency in mice results in cleft palate formation due to inhibition of the directional migration of cells that is required for palate formation [68]. Thus, the similarity of the craniofacial defects in *Wnt5a*^{-/-}, *Vangl2*^{Lp/Lp}, and *Dlgh-1*^{-/-} mice suggests that *Dlgh-1* may be a regulator of craniofacial skeletogenesis through a mechanism that involves modulating Wnt/PCP.

The *Dlgh-1*^{-/-} mice exhibited defects not only in skeletal structures of the head, but also of the trunk and limbs and the skeletons were reduced in size overall. In particular, the forelimbs and hindlimbs of *Dlgh-1*^{-/-} mice were approximately 20% shorter than those of *Dlgh-1*^{+/+} mice and the humerus was clearly wider in the mutants as compared to controls (Fig. 6). One possibility is that the reduced size is due to an inhibition of proliferation, as *Dlgh-1* has been associated with regulating proliferation [22]. However, Wnt/PCP also has been shown to play a role in limb development [69,70]. *Wnt5a* mutant mice exhibit truncated limbs [67] and the directional outgrowth of the limb has been shown to require *Wnt5a*/JNK signaling in the distal mesenchyme [71,72]. Similarly, *Vangl2*^{Lp/Lp} mice display shorter and wider limbs [73]. Recent studies have demonstrated a genetic and mechanistic link between *Wnt5a* and *Vangl2* through the frizzled-like receptor, *Ror2* [73], which binds *Wnt5a* [74], clearly establishing a connection between *Wnt5a* and a core PCP protein. Thus, the similarities in the limb phenotypes of these mouse mutants and the *Dlgh-1*^{-/-} mice combined with the known mechanistic link between *Dlgh-1* and *Vangl2* suggest that the mechanism through which *Dlgh-1* exerts its effects may be through modulating Wnt/PCP.

Although, the most likely explanation for the defects in skeletogenesis in the *Dlgh-1* mutant mice is that *Dlgh-1* is required the Wnt/PCP-dependent development of these skeletal structures, analysis of mouse mutants has demonstrated that numerous other signaling pathways play a role in skeletogenesis. These include FGFR [75,76], TGFβII [75,77], BMP [78], and Wnt/β-catenin [79,80,81,82]. Further studies will be required to determine if the mechanism through which *Dlgh-1* affects bone formation is through an effect on Wnt/PCP and how Wnt/PCP signaling coordinates with these other signaling pathways to direct the proper formation of the skeleton.

In summary, we provide evidence of new roles for *Dlgh-1* in the regulation of PCP and both endochondral and intramembranous bone formation in the mouse.

Materials and Methods

Ethics Statement

All procedures using mice conformed to the Guide for the Care and Use of Laboratory Animals of the National Institutes of

Health and the ARVO Statement for the Use of Animals in Ophthalmic and Vision Research. The protocol covering these studies (protocol #M00712) was approved by the Institutional Animal Care and Use Committee of the University of Wisconsin School of Medicine and Public Health (Animal Welfare Assurance #A3368-01).

Generation of the *Dlgh-1* Null Mouse

The generation of the mice carrying the gene targeted *Dlgh-1* conditional allele (Fig. 1A) has been described in detail previously (Rivera et al., 2009). To generate mice carrying a germline null mutation in *Dlgh-1*, female *Dlgh-1^{fl/+}* mice were mated to male *EIIA-Cre* transgenic mice [41] (Fig. 1). Removal of exon 8, which encodes a portion of the first PDZ domain of the Dlgh-1 protein, results in a frameshift mutation that generates a termination codon 3 codons downstream of the deletion. Male F1 progeny were mated to stock C57BL/6J or FVB/NJ females. Tail DNAs from the F2 progeny were screened by PCR for both the WT allele and the null allele using the Dlgh-1 5' primer CATCATGGTT-GAAGTGCTCTGGGC paired to the Dlgh-1 3' primer GGAAGGAACTCACGGATGGTCC (Fig. 1).

Gross and Microscopic Analyses

For examination of morphological defects at the gross level, newborn mice were examined for overt defects and photographed under a dissecting microscope. To examine palate formation, E18.5 mice were collected from pregnant dams and an incision made through the temporal-mandibular joint to expose the palate surface. Embryos were staged by designating the morning of the vaginal plug as day E0.5.

For histological analysis, E14.5, E16.5, and E18.5 embryos and neonates from *Dlgh-1^{+/+}*, *Dlgh-1^{+/-}*, and *Dlgh-1^{-/-}* animals were fixed in 4% paraformaldehyde at 4°C for 2–3 days, dehydrated through graded alcohols and xylenes, and embedded in paraffin for transverse, coronal, and sagittal sectioning. E18.5 day embryos were decalcified prior to dehydration. Serial 5 µm paraffin sections were stained with hematoxylin and eosin and viewed by light microscopy. For detection of Dlgh-1 protein by immunohistochemistry, transverse oriented sections from E15.5 embryos were rehydrated and stained with an anti-SAP97 antibody (1:500 dilution, obtained from J. Hell, University of Iowa), followed by Vectastain ABC-AP and Vector Red (Vector Labs) according to manufacturer's instructions. For detection of Dlgh-1 and Vangl2 proteins by immunofluorescence, sagittal sections from paraffin embedded newborn *Dlgh-1^{+/+}* and *Dlgh-1^{-/-}* mice were rehydrated, boiled in a rice cooker for 30 minutes in a solution of 10 mM Tris/1 mM EDTA/0.05% Tween-20 pH 9.0, blocked in 5% donkey serum diluted in 1X PBS, incubated with an anti-Dlgh-1 antibody (1:1000 dilution, catalog number NBP1-48054, Novus Biologicals) and an anti-Vangl2 antibody (1:100 dilution, catalog number sc-46560, Santa Cruz Biotechnology) overnight at 4°C. The next day, sections were washed and incubated with fluorescein conjugated horse anti-mouse and Alexa Fluor 568 conjugated goat anti-rabbit secondary antibodies for 1 hour at room temperature. Stained sections were viewed on a Zeiss Axioimager M2 microscope and images captured using Axiovision 4.8.2 software.

Cochlear Hair Cell Stereociliary Bundle Staining

The intact organ of Corti from E18.5 *Dlgh-1^{+/+}*, *Dlgh-1^{+/-}*, and *Dlgh-1^{-/-}* embryos was isolated in Hank's Balanced Salt Solution (HBSS, Gibco, Invitrogen) and fixed in 4% paraformaldehyde for 3 hours at 4°C. After initial fixation, the stria vascularis and tectorial membrane were removed and then the explants were

fixed in 4% paraformaldehyde for overnight at 4°C. The fixed explants were permeabilized with 0.5% triton-X100 in HBSS for 30 minutes at room temperature, then stained with Alexa Fluor 568-phalloidin (1 µg/ml, Molecular Probes) for 1 hour, and finally mounted as a surface preparation on a glass slide. Stained sections were viewed on a Nikon Diaphot 200 confocal microscope and images were captured using BioRad 1024 software. The orientation of individual stereociliary bundles was determined relative to a line parallel to the neural-abneural axis and perpendicular to the row of pillar cells, as described by Montcouquiol et al. [4]. The deviation from the neural-abneural axis was measured in degrees with a protractor. A cell with the vertex of the stereociliary bundle parallel to the neural-abneural axis was assigned 0° deviation. A total of 4 cochleae from 3 different mice of each genotype were analyzed. The data were subjected to statistical analysis using the two-sided Wilcoxon Rank Sums test and $p < .05$ was considered statistically significant. For detection of Dlgh-1 in the hair cells by immunofluorescence, fixed explants were immersed in 150 mM Tris-HCl, pH 9.0 at 65°C for 15 minutes followed by acetone treatment at -20°C for 20 minutes. After washing, explants were blocked in 10% serum diluted in 0.5% Triton X-100 in PBS for 2 hours at room temperature. Explants then were incubated with anti-Dlgh-1 antibody (1:500 dilution, Novus Biologicals) overnight at 4°C followed by incubation with fluorescein conjugated horse anti-mouse secondary antibody for 2 hours at room temperature. Immunostained explants were viewed and photographed as described above.

Immunoblot Analysis

Whole tissues and MEFs were lysed in RIPA Buffer [1% NP-40, 0.1% sodium dodecyl sulfate (SDS), 0.5% deoxycholate sodium (DOC), 150 mM NaCl, 50 mM Tris, pH 8.0] and centrifuged at 13,200 rpm for 15 minutes at 4°C. Protein concentrations in cell extracts were determined by the bicinchoninic acid (BCA) assay. Fifty µg of RIPA-soluble lysate from E18.5 *Dlgh-1^{+/+}*, *Dlgh-1^{+/-}*, and *Dlgh-1^{-/-}* animals were run on a 7.5% acrylamide gel and transferred to a PVDF membrane. The blots were blocked in 5% nonfat dry milk 1X PBS containing 0.1% Tween-20 and then incubated with mouse anti-Dlgh-1 (catalog number 610874, BD Transduction Laboratories), which was raised against amino acids 5–213 of human Dlgh-1 (amino acids upstream of the first PDZ domain), for 3 hours at room temperature in block solution. After washing and incubation with HRP-coupled goat-mouse (Pierce), detection was performed with ECL plus (Amersham). Blots were reprobed with mouse anti-β-actin (Sigma) as loading control.

Skeletal Staining

Eviscerated carcasses from E18.5 *Dlgh-1^{+/+}*, *Dlgh-1^{+/-}*, and *Dlgh-1^{-/-}* animals were fixed in 95% ethanol for 5 days at room temperature. After fixation, samples were cleared in 1% KOH for 2 days at RT. Samples were stained in 0.5% alcian blue 8GS (in 70% ethanol, 5% glacial acetic acid) and 0.2% alizarin red S solution (95% ethanol, 5% glacial acetic acid) for 5 days at room temperature. Samples were destained in 1% KOH for 2 days at room temperature and in graded glycerol/1% KOH at room temperature.

Acknowledgments

We thank the McArdle Laboratory Histology Core for tissue processing and the Keck Facility for confocal microscopy. We thank Heidi Rosenbaum and Malinda Waldof for technical assistance, Ruth Sullivan for helpful discussions on the histopathology of the *Dlgh-1^{-/-}* mice, and Robert Fettiplace for helpful discussions and insight.

Author Contributions

Conceived and designed the experiments: CR SJSS IFY SS MMN MB PFL AEG. Performed the experiments: CR SJSS IFY SS MMN MB.

References

- Woods DF, Hough C, Peel D, Callaini G, Bryant PJ (1996) Dlg protein is required for junction structure, cell polarity, and proliferation control in *Drosophila* epithelia. *J Cell Biol* 134: 1469–1482.
- Bilder D, Li M, Perrimon N (2000) Cooperative regulation of cell polarity and growth by *Drosophila* tumor suppressors. *Science* 289: 113–116.
- Wang Y, Nathans J (2007) Tissue/planar cell polarity in vertebrates: new insights and new questions. *Development* 134: 647–658.
- Montcouquiol M, Rachel RA, Lanford PJ, Copeland NG, Jenkins NA, et al. (2003) Identification of *Vangl2* and *Scrb1* as planar polarity genes in mammals. *Nature* 423: 173–177.
- Bossinger O, Klebes A, Segbert C, Theres C, Knust E (2001) Zonula adherens formation in *Caenorhabditis elegans* requires *dlg-1*, the homologue of the *Drosophila* gene discs large. *Dev Biol* 230: 29–42.
- Firestein BL, Rongo C (2001) DLG-1 is a MAGUK similar to SAP97 and is required for adherens junction formation. *Mol Biol Cell* 12: 3465–3475.
- Koppen M, Sims JS, Sims PA, Firestein BL, Hall DH, et al. (2001) Cooperative regulation of AJM-1 controls junctional integrity in *Caenorhabditis elegans* epithelia. *Nat Cell Biol* 3: 983–991.
- McMahon L, Legouis R, Vonesch JL, Labouesse M (2001) Assembly of *C. elegans* apical junctions involves positioning and compaction by LET-413 and protein aggregation by the MAGUK protein DLG-1. *J Cell Sci* 114: 2265–2277.
- Segbert C, Johnson K, Theres C, van Furden D, Bossinger O (2004) Molecular and functional analysis of apical junction formation in the gut epithelium of *Caenorhabditis elegans*. *Dev Biol* 266: 17–26.
- Bilder D (2001) PDZ proteins and polarity: functions from the fly. *Trends Genet* 17: 511–519.
- Bellaïche Y, Radovic A, Woods DF, Hough CD, Parmentier M-L, et al. (2001) The Partner of *Inscuteable/Discs-large* complex is required to establish planar polarity during asymmetric cell division in *Drosophila*. *Cell* 106: 355–366.
- Caruana G (2002) Genetic studies define MAGUK proteins as regulators of epithelial cell polarity. *Int J Dev Biol* 46: 511–518.
- Lin L, Sahr KE, Chishti AH (1997) Identification of the mouse homologue of human discs large and rat SAP97 genes. *Biochim Biophys Acta* 1362: 1–5.
- Lue RA, Marfatia SM, Branton D, Chishti AH (1994) Cloning and characterization of *hdlg*: the human homologue of the *Drosophila* discs large tumor suppressor binds to protein 4.1. *Proc Natl Acad Sci U S A* 91: 9818–9822.
- Muller BM, Kistner U, Veh RW, Cases-Langhoff C, Becker B, et al. (1995) Molecular characterization and spatial distribution of SAP97, a novel presynaptic protein homologous to SAP90 and the *Drosophila* discs-large tumor suppressor protein. *J Neurosci* 15: 2354–2366.
- McLaughlin M, Hale R, Elliston D, Gaudet S, Lue RA, et al. (2002) The distribution and function of alternatively spliced insertions in *hDlg*. *J Biol Chem* 277: 6406–6412.
- Nguyen MM, Rivera C, Griep AE (2005) Localization of PDZ domain containing proteins Discs Large-1 and Scribble in the mouse eye. *Mol Vis* 11: 1183–1199.
- Thomas U, Phannavong B, Muller B, Garner CC, Gundelfinger ED (1997) Functional Expression of Rat Synapse-Associated Proteins Sap97 and Sap102 in *Drosophila* Dlg-1 Mutants - Effects On Tumor Suppression and Synaptic Bouton Structure. *Mech Dev* 62: 161–174.
- Rafael JA, Hutchinson TL, Lumeng CN, Marfatia SM, Chishti AH, et al. (1998) Localization of Dlg at the mammalian neuromuscular junction. *Neuroreport* 9: 2121–2125.
- Laprise P, Viel A, Rivard N (2004) Human homolog of disc-large is required for adherens junction assembly and differentiation of human intestinal epithelial cells. *J Biol Chem* 279: 10157–10166.
- Dow LE, Brumby AM, Muratore R, Coombe ML, Sedelies KA, et al. (2003) *hScrib* is a functional homologue of the *Drosophila* tumour suppressor Scribble. *Oncogene* 22: 9225–9230.
- Ishidate T, Matsumine A, Toyoshima K, Akiyama T (2000) The APC-hDLG complex negatively regulates cell cycle progression from the G0/G1 to S phase. *Oncogene* 19: 365–372.
- Valiente M, Andres-Pons A, Gomar B, Torres J, Gil A, et al. (2005) Binding of PTEN to specific PDZ domains contributes to PTEN protein stability and phosphorylation by microtubule-associated serine/threonine kinases. *J Biol Chem* 280: 28936–28943.
- Kim E, Niethammer M, Rothschild A, Jan YN, Sheng M (1995) Clustering of Shaker-type K⁺ channels by interaction with a family of membrane-associated guanylate kinases. *Nature* 378: 85–88.
- Yamamoto Y, Irie K, Asada M, Mino A, Mandai K, et al. (2004) Direct binding of the human homologue of the *Drosophila* disc large tumor suppressor gene to seven-pass transmembrane proteins, tumor endothelial marker 5 (TEM5), and a novel TEM5-like protein. *Oncogene* 23: 3889–3897.
- Lee S, Fan S, Makarova O, Straight S, Margolis B (2002) A novel and conserved protein-protein interaction domain of mammalian Lin-2/CASK binds and recruits SAP97 to the lateral surface of epithelia. *Mol Cell Biol* 22: 1778–1791.
- Kiyono T, Hiraiwa A, Fujita M, Hayashi Y, Akiyama T, et al. (1997) Binding of high-risk human papillomavirus E6 oncoproteins to the human homologue of the *Drosophila* discs large tumor suppressor protein. *Proc Natl Acad Sci U S A* 94: 11612–11616.
- Lee SS, Weiss RS, Javier RT (1997) Binding of human virus oncoproteins to hDlg/SAP97, a mammalian homolog of the *Drosophila* discs large tumor suppressor protein. *Proc Natl Acad Sci U S A* 94: 6670–6675.
- Suzuki T, Ohsugi Y, Uchida-Toita M, Akiyama T, Yoshida M (1999) Tax oncoprotein of HTLV-1 binds to the human homologue of *Drosophila* discs large tumor suppressor protein, hDLG, and perturbs its function in cell growth control. *Oncogene* 18: 5967–5972.
- Shai A, Brake T, Somoza C, Lambert PF (2007) The human papillomavirus E6 oncoprotein dysregulates the cell cycle and contributes to cervical carcinogenesis through two independent activities. *Cancer Res* 67: 1626–1635.
- Frese KK, Latorre JJ, Chung SH, Caruana G, Bernstein A, et al. (2006) Oncogenic function for the Dlg1 mammalian homolog of the *Drosophila* discs-large tumor suppressor. *Embo J* 25: 1406–1417.
- Simonson SJ, Difilippantonio MJ, Lambert PF (2005) Two distinct activities contribute to human papillomavirus 16 E6's oncogenic potential. *Cancer Res* 65: 8266–8273.
- Hirata A, Higuchi M, Niinuma A, Ohashi M, Fukushi M, et al. (2004) PDZ domain-binding motif of human T-cell leukemia virus type 1 Tax oncoprotein augments the transforming activity in a rat fibroblast cell line. *Virology* 318: 327–336.
- Caruana G, Bernstein A (2001) Craniofacial dysmorphogenesis including cleft palate in mice with an insertional mutation in the discs large gene. *Mol Cell Biol* 21: 1475–1483.
- Naim E, Bernstein A, Bertram JF, Caruana G (2005) Mutagenesis of the epithelial polarity gene, discs large 1, perturbs nephrogenesis in the developing mouse kidney. *Kidney Int* 68: 955–965.
- Nguyen MM, Nguyen ML, Caruana G, Bernstein A, Lambert PF, et al. (2003) Requirement of PDZ-containing proteins for cell cycle regulation and differentiation in the mouse lens epithelium. *Mol Cell Biol* 23: 8970–8981.
- Feng W, Long JF, Fan JS, Suetake T, Zhang M (2004) The tetrameric L27 domain complex as an organization platform for supramolecular assemblies. *Nat Struct Mol Biol* 11: 475–480.
- Mahoney ZX, Sammut B, Xavier RJ, Cunningham J, Go G, et al. (2006) Discs-large homolog 1 regulates smooth muscle orientation in the mouse ureter. *Proc Natl Acad Sci U S A* 103: 19872–19877.
- Iizuka-Kogo A, Ishidao T, Akiyama T, Senda T (2007) Abnormal development of urogenital organs in *Dlgh1*-deficient mice. *Development* 134: 1799–1807.
- Rivera C, Yamben IF, Shatadal S, Waldof M, Robinson ML, et al. (2009) Cell-autonomous requirements for Dlg-1 for lens epithelial cell structure and fiber cell morphogenesis. *Dev Dyn* 238: 2292–2308.
- Lakso M, Pichel JG, Gorman JR, Sauer B, Okamoto Y, et al. (1996) Efficient in vivo manipulation of mouse genomic sequences at the zygote stage. *Proc Natl Acad Sci U S A* 93: 5860–5865.
- Murdoch JN, Henderson DJ, Doudney K, Gaston-Massuet C, Phillips HM, et al. (2003) Disruption of scribble (*Scrb1*) causes severe neural tube defects in the circletail mouse. *Hum Mol Genet* 12: 87–98.
- Rachel RA, Murdoch JN, Beermann F, Copp AJ, Mason CA (2000) Retinal axon misrouting at the optic chiasm in mice with neural tube closure defects. *Genesis* 27: 32–47.
- Murdoch JN, Doudney K, Paternotte C, Copp AJ, Stanier P (2001) Severe neural tube defects in the loop-tail mouse result from mutation of *Lpp1*, a novel gene involved in floor plate specification. *Hum Mol Genet* 10: 2593–2601.
- Torban E, Wang HJ, Patenaude AM, Riccomagno M, Daniels E, et al. (2007) Tissue, cellular and sub-cellular localization of the *Vangl2* protein during embryonic development: effect of the *Lp* mutation. *Gene Expr Patterns* 7: 346–354.
- Murdoch JN, Rachel RA, Shah S, Beermann F, Stanier P, et al. (2001) Circletail, a new mouse mutant with severe neural tube defects: chromosomal localization and interaction with the loop-tail mutation. *Genomics* 78: 55–63.
- Keller R (2002) Shaping the vertebrate body plan by polarized embryonic cell movements. *Science* 298: 1950–1954.
- Dabdoub A, Donohue MJ, Brennan A, Wolf V, Montcouquiol M, et al. (2003) Wnt signaling mediates reorientation of outer hair cell stereociliary bundles in the mammalian cochlea. *Development* 130: 2375–2384.
- Hartmann C (2006) A Wnt canon orchestrating osteoblastogenesis. *Trends Cell Biol* 16: 151–158.
- Qian D, Jones C, Rzedzinska A, Mark S, Zhang X, et al. (2007) Wnt5a functions in planar cell polarity regulation in mice. *Dev Biol* 306: 121–133.

51. Kibar Z, Vogan KJ, Groulx N, Justice MJ, Underhill DA, et al. (2001) Ltap, a mammalian homolog of *Drosophila* Strabismus/Van Gogh, is altered in the mouse neural tube mutant Loop-tail. *Nat Genet* 28: 251–255.
52. Wang J, Hamblet NS, Mark S, Dickinson ME, Brinkman BC, et al. (2006) Dishevelled genes mediate a conserved mammalian PCP pathway to regulate convergent extension during neurulation. *Development* 133: 1767–1778.
53. Wang Y, Guo N, Nathans J (2006) The role of Frizzled3 and Frizzled6 in neural tube closure and in the planar polarity of inner-ear sensory hair cells. *J Neurosci* 26: 2147–2156.
54. Curtin JA, Quint E, Tspouri V, Arkel RM, Cattanach B, et al. (2003) Mutation of *Celsr1* disrupts planar polarity of inner ear hair cells and causes severe neural tube defects in the mouse. *Curr Biol* 13: 1129–1133.
55. Lu X, Borchers AG, Jolicoeur C, Rayburn H, Baker JC, et al. (2004) PTK7/CCK-4 is a novel regulator of planar cell polarity in vertebrates. *Nature* 430: 93–98.
56. Montcouquiol M, Sans N, Huss D, Kach J, Dickman JD, et al. (2006) Asymmetric localization of Vangl2 and Fz3 indicate novel mechanisms for planar cell polarity in mammals. *J Neurosci* 26: 5265–5275.
57. Yao R, Natsume Y, Noda T (2004) MAGI-3 is involved in the regulation of the JNK signaling pathway as a scaffold protein for frizzled and Ltap. *Oncogene* 23: 6023–6030.
58. Hering H, Sheng M (2002) Direct interaction of Frizzled-1, -2, -4, and -7 with PDZ domains of PSD-95. *FEBS Lett* 521: 185–189.
59. Wawrzak D, Luyten A, Lambaerts K, Zimmermann P (2009) Frizzled-PDZ scaffold interactions in the control of Wnt signaling. *Adv Enzyme Regul* 49: 98–106.
60. Van Campenhout CA, Eitelhuber A, Gloeckner CJ, Giallonardo P, Gegg M, et al. (2011) Dlg3 trafficking and apical tight junction formation is regulated by Nedd4 and Nedd4-2 E3 ubiquitin ligases. *Dev Cell* 21: 479–491.
61. Bastock R, Strutt H, Strutt D (2003) Strabismus is asymmetrically localised and binds to Prickle and Dishevelled during *Drosophila* planar polarity patterning. *Development* 130: 3007–3014.
62. Park M, Moon RT (2002) The planar cell-polarity gene *stbm* regulates cell behaviour and cell fate in vertebrate embryos. *Nat Cell Biol* 4: 20–25.
63. Topczewski J, Dale RM, Sisson BE (2011) Planar cell polarity signaling in craniofacial development. *Organogenesis* 7: 255–259.
64. Bekman E, Henrique D (2002) Embryonic expression of three mouse genes with homology to the *Drosophila melanogaster* prickle gene. *Mech Dev* 119 Suppl 1: S77–81.
65. Darken RS, Scola AM, Rakeman AS, Das G, Mlodzik M, et al. (2002) The planar polarity gene *strabismus* regulates convergent extension movements in *Xenopus*. *EMBO J* 21: 976–985.
66. De Calisto J, Araya C, Marchant L, Riaz CF, Mayor R (2005) Essential role of non-canonical Wnt signalling in neural crest migration. *Development* 132: 2587–2597.
67. Yamaguchi TP, Bradley A, McMahon AP, Jones S (1999) A Wnt5a pathway underlies outgrowth of multiple structures in the vertebrate embryo. *Development* 126: 1211–1223.
68. He F, Xiong W, Yu X, Espinoza-Lewis R, Liu C, et al. (2008) Wnt5a regulates directional cell migration and cell proliferation via Ror2-mediated noncanonical pathway in mammalian palate development. *Development* 135: 3871–3879.
69. Barrow J (2011) Wnt/planar cell polarity signaling: an important mechanism to coordinate growth and patterning in the limb. *Organogenesis* 7: 260–266.
70. Romerim SM, Dudley AT (2011) Cell polarity: The missing link in skeletal morphogenesis? *Organogenesis* 7: 217–228.
71. Wyngaarden LA, Vogeli KM, Ciruna BG, Wells M, Hadjantonakis AK, et al. (2010) Oriented cell motility and division underlie early limb bud morphogenesis. *Development* 137: 2551–2558.
72. Gros J, Hu JK, Vinegoni C, Feruglio PF, Weissleder R, et al. (2010) WNT5A/JNK and FGF/MAPK pathways regulate the cellular events shaping the vertebrate limb bud. *Curr Biol* 20: 1993–2002.
73. Wang B, Sinha T, Jiao K, Serra R, Wang J (2011) Disruption of PCP signaling causes limb morphogenesis and skeletal defects and may underlie Robinow syndrome and brachydactyly type B. *Hum Mol Genet* 20: 271–285.
74. Gao B, Song H, Bishop K, Elliot G, Garrett L, et al. (2011) Wnt signaling gradients establish planar cell polarity by inducing Vangl2 phosphorylation through Ror2. *Dev Cell* 20: 163–176.
75. Sasaki T, Ito Y, Bringas P, Jr., Chou S, Urata MM, et al. (2006) TGFbeta-mediated FGF signaling is crucial for regulating cranial neural crest cell proliferation during frontal bone development. *Development* 133: 371–381.
76. Trokovic N, Trokovic R, Mai P, Partanen J (2003) Fgfr1 regulates patterning of the pharyngeal region. *Genes Dev* 17: 141–153.
77. Ito Y, Yeo JY, Chytil A, Han J, Bringas P, Jr., et al. (2003) Conditional inactivation of Tgfb2 in cranial neural crest causes cleft palate and calvaria defects. *Development* 130: 5269–5280.
78. Dudas M, Sridurongrit S, Nagy A, Okazaki K, Kaartinen V (2004) Craniofacial defects in mice lacking BMP type I receptor Alk2 in neural crest cells. *Mech Dev* 121: 173–182.
79. Brault V, Moore R, Kutsch S, Ishibashi M, Rowitch DH, et al. (2001) Inactivation of the beta-catenin gene by Wnt1-Cre-mediated deletion results in dramatic brain malformation and failure of craniofacial development. *Development* 128: 1253–1264.
80. Day TF, Guo X, Garrett-Beal L, Yang Y (2005) Wnt/beta-catenin signaling in mesenchymal progenitors controls osteoblast and chondrocyte differentiation during vertebrate skeletogenesis. *Dev Cell* 8: 739–750.
81. Hill TP, Spater D, Taketo MM, Birchmeier W, Hartmann C (2005) Canonical Wnt/beta-catenin signaling prevents osteoblasts from differentiating into chondrocytes. *Dev Cell* 8: 727–738.
82. Joeng KS, Schumacher CA, Zylstra-Diegel CR, Long F, Williams BO (2011) Lrp5 and Lrp6 redundantly control skeletal development in the mouse embryo. *Dev Biol* 359: 222–229.